Polarization attributes of stimulated Brillouin scattering slow light in fiber

Avi Zadok*[a], Avishay Eyal[b], Moshe Tur[b], and Luc Thevenaz[c]
[a]School of Engineering, Bar-Ilan University, Ramat-Gan 52900,Israel;
[b]Faculty of Engineering, Tal-Aviv University, Tel-Aviv 69978, Israel;
[c]Institute of Electrical Engineering, Ecole Polytechnique Fédérale de Lausanne, STI-GR-SCI Station 11, 1015 Lausanne, Switzerland.

ABSTRACT

The polarization-related properties of stimulated Brillouin scattering (SBS) processes in long, randomly birefringent, standard optical fibers are examined. Evolution equations for the pump and signal waves, in the presence of both birefringence and SBS, are provided in Jones and Stokes spaces. It is shown that in the undepleted pump regime, the amplification of the SBS signal wave is equivalent to that of a linear medium with polarization-dependent gain. The process is associated with a pair of orthogonal states of polarizations (SOPs) of the signal wave, which undergo maximum and minimum amplification. In long, standard fibers, the Jones vector of the probe SOP which corresponds to maximum amplification is aligned with the complex conjugate of the pump wave Jones vector. The maximum and minimum SBS gain coefficients in such fibers equal two-thirds and one-third of the gain coefficient that is predicted by scalar theory, respectively. The large differential gain of the SBS process gives rise to an effective pulling of the amplified Stokes probe wave SOP, towards that of maximum amplification. Lastly, Stokes wave pulses that are aligned for maximum and minimum amplification experience different group delays, which manifest as polarization-related distortions in SBS slow light setups.

Keywords: Stimulated Brillouin scattering, slow and fast light, polarimetry, nonlinear fiber optics

1. INTRODUCTION

Stimulated Brillouin Scattering (SBS) requires the lowest activation power of all non-linear effects in silica optical fibers. In SBS, a strong pump wave and a typically weak, counter-propagating signal wave optically interfere to generate, through electrostriction, a traveling longitudinal acoustic wave. The acoustic wave, in turn, couples these optical waves to each other[1, 2]. The SBS interaction is efficient only when the difference between the optical frequencies of the pump and signal waves is very close (within a few tens of MHz) to a fiber-dependent parameter, the Brillouin shift ν_B, which is of the order of 10-11 GHz in silica fibers at room temperature and at telecommunication wavelengths[1, 2]. An input signal whose frequency is ν_B lower than that of the pump (Stokes wave) experiences SBS amplification. If the input signal frequency is ν_B above that of the pump (anti-Stokes wave), SBS-induced signal attenuation is obtained instead. The strength of the interaction is often quantified in terms of an exponential gain coefficient γ, which is defined as the logarithm of the signal linear power gain (or loss), normalized to a unit pump power and unit fiber length $[\mathrm{W}\cdot\mathrm{m}]^{-1}$.

SBS has found numerous applications, including distributed sensing of temperature and strain[3-5], fiber lasers[6], optical processing of high frequency microwave signals[7-11], and even optical memories[12]. The SBS amplification (or attenuation) is accompanied by frequency dependent phase delays[1], which modify the group delay of signal pulses. SBS has become a favorable underlying mechanism in many such variable group delay setups, often referred to as *slow and fast light*, for its low threshold power, robustness and simplicity of operation[13-20].

Since SBS originates from optical interference between the pump and signal waves, the SBS interaction, at a given point along the fiber, is most efficient when the electric fields of the pump and signal are aligned, i.e., their vectors trace parallel ellipses and in the same sense of rotation. Conversely, if the two ellipses are again similar, but traced in opposite

* zadoka@eng.biu.ac.il Tel.: +972-3-5318882; Fax: +972-3-7384051.

Advances in Slow and Fast Light IV, edited by Selim M. Shahriar, Philip R. Hemmer,
Proc. of SPIE Vol. 7949, 79490A · © 2011 SPIE · CCC code: 0277-786X/11/$18
doi: 10.1117/12.880790

senses of rotation, with their long axes being orthogonal to each other, then the SBS interaction at that point averages to zero over an optical period. Consequently, in the presence of birefringence, both the local and the overall signal gain (or loss) depends on the birefringent properties of the fiber, as well as on the input states of polarization (SOPs) of both pump and signal. Following initial work by Horiguchi *et al*.[21], van Deventer and Boot[22] have studied in detail the signal SOPs leading to maximum and minimum gain. Based on the statistical properties of the evolution of the pump and signal SOPs in sufficiently long fibers, they argued that for standard, low birefringence fibers the maximum gain coefficient is twice that of the minimum one, and equals 2/3 of the maximum gain coefficient in a birefringence-free fiber γ_0. Furthermore, maximum gain is achieved when the pump and signal have identical polarizations (in their respective directions of propagation), while minimum gain is obtained for the corresponding 'orthogonal' case* [23-24]. Their analysis was nicely corroborated by an experiment. However, the SBS amplification of an arbitrarily polarized input signal SOP was not discussed, nor was the role played by the Brillouin effect itself in the evolution of the signal SOP considered.

In this work, the study of van Deventer and Boot is analytically substantiated and extended, using a vector formulation of the SBS amplification process in the presence of birefringence. A vector differential equation, combining both effects, is studied in the Jones and Stokes spaces. The analysis shows that in the undepleted pump regime, the SBS-amplifying fiber is equivalent to a polarization dependent gain medium. The maximum and minimum gains in that medium are associated with a pair of orthogonal signal SOPs[25]. These maximum and minimum gain SOPs provide a convenient vector base for the examination of arbitrarily polarized input signal waves. In sufficiently long standard fibers, these two SOPs are governed by the launch SOP of the pump wave alone, and do not depend on the birefringence properties of the specific fiber. In addition, we show that the evolution of the signal SOP is controlled not only by the fiber birefringence but also by the local SBS interaction, which drags the signal SOP towards that of the pump. Consequently, the output SOP of an amplified Stokes wave is seen to converge towards a specific, preferred state, that of maximum amplification, which is practically independent of both the input signal SOP and polarization transformations along the fiber[25]. The preferred output SOP could be arbitrarily varied, however, by changing the input pump SOP. The SOP of an attenuated anti-Stokes wave, on the other hand, is repelled from the same specific SOP. Such *polarization pulling* is experimentally demonstrated for both Stokes and anti-Stokes signals.

In SBS slow-light setups, pulse distortion due to the limited bandwidth and the dispersion associated with the scalar frequency dependence of SBS has been thoroughly documented[26]. In the final part of this work, we show that SBS-related, polarization-induced distortion is yet another mechanism responsible for pulse broadening in slow light setups. A signal pulse with its SOP aligned for maximum amplification undergoes a delay much longer than that experienced by a pulse whose SOP is adjusted for minimum gain. Thus, the resulting distortion is analogous to that of linear birefringence, where the orthogonal SOPs of maximum and minimum gain have a similar role to that of the principal axes in linear birefringence induced polarization mode dispersion (PMD)[27]. The broadening due to polarization of moderately delayed signal pulses could exceed that of pulses aligned for maximum delay. Polarization-induced distortion in an SBS slow light setup is shown experimentally as well.

The remainder of this paper is organized as follows. Section 2 provides the analysis of SBS amplification in standard, weakly birefringent fibers. Both continuous wave (CW) and pulsed signals are considered. Experimental demonstration of SBS polarization pulling and measurements of polarization-induced distortion in SBS slow light are given in section 3. Concluding remarks are provided in section 4.

* In the work of van Deventer and Boot[22], the pump and probe SOPs are defined in two different reference frames, corresponding to opposite directions of propagation. In this work, as well as in most of the literature on polarization[23-24], a single reference frame is used. Therefore, we defer the mathematical description of the conditions for maximum/minimum SBS gain to the next section.

2. ANALYSIS OF STIMULATED BRILLOUIN SCATTERING IN BIREFRINGENT FIBERS

2.1 Propagation equations of the signal wave in Jones and Stokes spaces

Let us denote the column Jones vector of a monochromatic signal wave as $\vec{E}_{sig}(z)$, z indicating position along the fiber, with the launch and exit points at $z=0$ and $z=L$, respectively (L is the fiber length). With no pump, the propagation of $\vec{E}_{sig}(z)$ can be described by:

$$\vec{E}_{sig}(z)=\mathbf{T}(z)\vec{E}_{sig}(0), \tag{1}$$

with $\mathbf{T}(z)$ a unitary Jones matrix representing the effect of fiber birefringence. The pump wave, whose Jones vector is denoted by $\vec{E}_{pump}(z)$, is launched into the fiber at $z=L$. Throughout this paper, we work in the same right-handed coordinate system $\{x,y,z\}$, where the signal propagates in the positive z direction, while the pump propagates in the negative z direction. Thus, if both $\vec{E}_{sig}(z)$ and $\vec{E}_{pump}(z)$ equal the 2X1 vector $[1\ j]^T$ (T stand for transpose), they represent a right-handed circularly polarized signal and a left-handed circularly polarized pump wave, respectively[23-24]. We neglect linear polarization-dependent power losses in the fiber, although such losses can be easily included in the analysis. Further, since the Brillouin shift ν_B is merely ~10GHz, and only a few kilometers of modern fibers are concerned, polarization mode dispersion can be ignored and, therefore, shifting the optical frequency by ν_B has a negligible effect on the Jones matrix of the fiber. Hence, the propagation of the pump wave (in the absence of a probe) can also be expressed using $\mathbf{T}(z)$:

$$\vec{E}_{pump}(0)=\mathbf{T}^T(z)\vec{E}_{pump}(z)\rightarrow\vec{E}_{pump}(z)=\mathbf{T}^*(z)\vec{E}_{pump}(0)\ ; \tag{2}$$

where $\text{inv}\left[\mathbf{T}^T(z)\right]=\mathbf{T}^*(z)$.

When both the probe and pump waves are present, the local evolution of $\vec{E}_{sig}(z)$ and $\vec{E}_{pump}(z)$ is driven by both the fiber birefringence and the SBS effect to give[27-28]:

$$\frac{d\vec{E}_{sig}(z)}{dz}=\left[\frac{d\mathbf{T}(z)}{dz}\mathbf{T}^{\dagger}(z)+\frac{\gamma_0}{2}\vec{E}_{pump}(z)\vec{E}^{\dagger}_{pump}(z)\right]\vec{E}_{sig}(z), \tag{3a}$$

$$\frac{d\vec{E}_{pump}(z)}{dz}=\left[\frac{d\mathbf{T}^*(z)}{dz}\mathbf{T}^{T}(z)+\frac{\gamma_0}{2}\vec{E}_{sig}(z)\vec{E}^{\dagger}_{sig}(z)\right]\vec{E}_{pump}(z). \tag{3b}$$

γ_0 $[\text{W}\cdot\text{m}]^{-1}$ is the SBS gain per unit length per a unit of pump power for a scalar interaction (i.e., for a fiber with no birefringence), and depends on the fiber material properties, the mode field diameter, the pump optical spectrum and the frequency offset between the pump and signal waves. We dedicate most of the analysis to the Stokes wave scenario, so that γ_0 is positive, but the analysis and results, properly interpreted, are equally valid for the anti-Stokes case, where the optical frequency of the signal is ν_B above that of the pump. The anti-Stokes signal surrenders its power to the pump, thereby becoming attenuated with an SBS attenuation coefficient of $-\gamma_0$. Note that $(\gamma_0/2)\left[\vec{E}_{pump}(z)\vec{E}^{\dagger}_{pump}(z)\right]$ is a 2×2 matrix, representing the outer product of a column vector ($\vec{E}_{pump}(z)$) with a row one (the transpose conjugate of $\vec{E}_{pump}(z)$).

From now on it will be assumed that SBS-induced signal amplification or attenuation negligibly affects the pump (i.e., the so-called undepleted pump approximation). Thus, the SBS term in Eq. (3b) can be ignored and Eq. (3a) becomes linear in $\vec{E}_{sig}(z)$. Therefore,

$$\vec{E}_{sig}(L) = \mathbf{H} \cdot \vec{E}_{sig}(0), \tag{4}$$

where $\mathbf{H}$ is a 2×2 matrix, which depends on the fiber birefringence, the fiber length L, the pump power, and its SOP at $z = L$. The matrix $\mathbf{H}$ is generally non-unitary. Nevertheless, it can be processed using the singular value decomposition (SVD) technique:

$$\mathbf{H} = \mathbf{U} \cdot \mathbf{S} \cdot \mathbf{V}^{\dagger} = \mathbf{U} \cdot \begin{bmatrix} G_1 & 0 \\ 0 & G_2 \end{bmatrix} \cdot \mathbf{V}^{\dagger}, \tag{5}$$

where $\mathbf{U}$ and $\mathbf{V}$ are unitary matrices, G_1, G_2 are real and positive and satisfy $G_1 > G_2 > 1$ in the case of SBS amplification and $1 > G_1 > G_2$ in the case of SBS attenuation. Using this decomposition two orthogonal input signal Jones vectors can be identified, which provide the maximum and minimum signal output powers, namely:

$$\vec{E}_{sig}^{in\_\max} = \left[\mathbf{V}^{\dagger}\right]^{-1} \begin{bmatrix} 1 \\ 0 \end{bmatrix} = \mathbf{V} \begin{bmatrix} 1 \\ 0 \end{bmatrix}; \quad \vec{E}_{sig}^{in\_\min} = \mathbf{V} \begin{bmatrix} 0 \\ 1 \end{bmatrix}. \tag{6}$$

The corresponding output Jones vectors are given by:

$$\vec{E}_{sig}^{out\_\max} = \mathbf{U} \cdot \mathbf{S} \cdot \mathbf{V}^{\dagger} \cdot \mathbf{V} \begin{bmatrix} 1 \\ 0 \end{bmatrix} = \mathbf{U} \cdot \mathbf{S} \begin{bmatrix} 1 \\ 0 \end{bmatrix} = G_1 \mathbf{U} \begin{bmatrix} 1 \\ 0 \end{bmatrix}, \ \vec{E}_{sig}^{out\_\min} = \mathbf{U} \cdot \mathbf{S} \cdot \mathbf{V}^{\dagger} \cdot \mathbf{V} \begin{bmatrix} 0 \\ 1 \end{bmatrix} = \mathbf{U} \cdot \mathbf{S} \begin{bmatrix} 0 \\ 1 \end{bmatrix} = G_2 \mathbf{U} \begin{bmatrix} 0 \\ 1 \end{bmatrix}, \tag{7}$$

and are, therefore, also orthogonal. It is thus convenient to represent an arbitrarily polarized input signal using the orthogonal base of $\vec{E}_{sig}^{in\_\max}$, $\vec{E}_{sig}^{in\_\min}$:

$$\vec{E}_{sig}^{in} = \alpha_0 \vec{E}_{sig}^{in\_\max} + \beta_0 \vec{E}_{sig}^{in\_\min}. \tag{8}$$

Using Equations. (7) and (8), the output signal Jones vector and the signal power are:

$$\vec{E}_{sig}^{out} = \alpha_0 G_1 \mathbf{U} \begin{bmatrix} 1 \\ 0 \end{bmatrix} + \beta_0 G_2 \mathbf{U} \begin{bmatrix} 0 \\ 1 \end{bmatrix}; \ P_{sig}^{out} = |\alpha_0|^2 G_1^2 + |\beta_0|^2 G_2^2. \tag{9}$$

When $G_1 >> G_2$, Eq. (9) suggests that unless α_0 is negligible, an arbitrarily polarized input signal will be drawn towards the SOP of $\vec{E}_{sig}^{out\_\max}$.

Next, we try to relate $\vec{E}_{sig}^{in\_\max}$, $\vec{E}_{sig}^{in\_\min}$ to the SOP of the pump wave. To that end, we have transformed Equations (3a) to the Stokes space[25]:

$$\frac{dS_{0\_sig}(z)}{dz} = \frac{\gamma_0 P_{pump}(z)}{2} \left(1 + \hat{s}_{pump}(z) \cdot \hat{s}_{sig}(z)\right) S_{0\_sig}(z), \tag{10a}$$

$$\begin{aligned} \frac{d\hat{s}_{sig}(z)}{dz} &= \vec{\beta}(z) \times \hat{s}_{sig}(z) + \frac{\gamma_0 P_{pump}(z)}{2} \hat{s}_{sig}(z) \times \left(\hat{s}_{pump}(z) \times \hat{s}_{sig}(z)\right) \\ &= \vec{\beta}(z) \times \hat{s}_{sig}(z) + \frac{\gamma_0 P_{pump}(z)}{2} \left[\hat{s}_{pump}(z) - \left(\hat{s}_{pump}(z) \cdot \hat{s}_{sig}(z)\right) \hat{s}_{sig}(z)\right] \end{aligned} \tag{10b}$$

Here S_{0_sig} is the signal power, $\hat{s}_{sig} = \left[s_{1,sig} \quad s_{2,sig} \quad s_{3,sig}\right]^T$ and similarly $\hat{s}_{pump}$ are 3X1 normalized Stokes vectors, describing the evolution of the polarizations of the counter-propagating signal and pump waves, respectively. Finally, P_{pump} denotes the pump power, which for the undepleted, lossless case is *z*-independent. The three-dimensional vector $\vec{\beta}(z)$ describes the fiber birefringence in Stokes space[27]:

$$\vec{\beta} \cdot \vec{\sigma} \equiv 2j \frac{d\mathbf{T}}{dz} \mathbf{T}^{\dagger}, \tag{11}$$

where $\vec{\sigma}$ is a row vector of Pauli spin matrices[27]. The vector $\vec{\beta}(z)$ is aligned with the Stokes space representation of the local slow axis of birefringence[27]. Note again that we express both Stokes vectors in the same right handed coordinate system, in which the signal wave propagates in the positive z direction. Therefore, the Stokes vector $\hat{s} = \begin{bmatrix} 0 & 0 & 1 \end{bmatrix}^T$ represents a right-handed circular polarization for the signal wave, but a left-handed circular polarization for the pump.

2.2 States of polarization for maximum and minimum amplification in long, standard fibers

Eq. (10a) is easily cast into a form:

$$\frac{d\ln\left(S_{0\_sig}\right)}{dz} = \frac{\gamma_0 P_{pump}(z)}{2}\left(1 + \hat{s}_{pump}\cdot\hat{s}_{sig}\right). \tag{12}$$

In the undepleted pump regime, the solution is readily obtained:

$$S_{0\_sig}^{out} = S_{0\_sig}^{in}\exp\left[\frac{\gamma_0 P_{pump}}{2}\int_0^L\left(1+\hat{s}_{pump}\cdot\hat{s}_{sig}\right)dz'\right] = S_{0\_sig}^{in}\exp\left[\frac{\gamma_0 P_{pump}}{2}L\left(1+\left\langle\hat{s}_{pump}\cdot\hat{s}_{sig}\right\rangle_L\right)\right]. \tag{13}$$

$\left\langle\hat{s}_{pump}\cdot\hat{s}_{sig}\right\rangle_L$ is the scalar product of the pump and signal Stokes vectors, averaged over the fiber length. Thus, for any input SOP one can define an effective SBS gain, given by:

$$\gamma = \frac{\gamma_0}{2}\left(1+\left\langle\hat{s}_{pump}\cdot\hat{s}_{sig}\right\rangle_L\right). \tag{14}$$

Obviously, γ depends on the input SOPs of both pump and signal.

Eq. (10b) specifies two driving forces that control the evolution of the SOP along the fiber. The first, $\vec{\beta}\times\hat{s}_{sig}$, describes the birefringence-induced evolution of the signal SOP[27]. The same term also governs the evolution of the pump SOP, albeit in the opposite direction. The second term, $(\gamma_0/2)P_{pump}\left[\hat{s}_{pump} - \left(\hat{s}_{pump}\cdot\hat{s}_{sig}\right)\hat{s}_{sig}\right]$, represents the effect of SBS amplification on the signal SOP. This second term has the following interpretation on the Poincare sphere: it is a vector, orthogonal to $\hat{s}_{sig}$, and tangentially (on the sphere surface) pointing towards $\hat{s}_{pump}$. This term signifies a force pulling $\hat{s}_{sig}$ towards $\hat{s}_{pump}$. The magnitude of this pulling force scales with the pump power and depends on the local projection of $\hat{s}_{pump}(z)$ on $\hat{s}_{sig}(z)$, vanishing when $\hat{s}_{sig}$ is either parallel to $\hat{s}_{pump}$ (pump and signal SOPs aligned) or anti-parallel to it (in the Stokes space, namely: orthogonal in the Jones space).

We now turn to the prevalent scenario of standard single-mode fibers, where the birefringence term Eq. (10b) is larger than the SBS term (for a an average beat length of 40 m, $\left\langle\left|\vec{\beta}\right|\right\rangle_z \sim 0.16\ \mathrm{m}^{-1}$ whereas $\gamma_0 P_{pump}/2 \sim 0.01\mathrm{m}^{-1}$ for $\gamma_0 = 0.2\left[\mathrm{m}\cdot\mathrm{W}\right]^{-1}$, $P_{pump} = 0.1\mathrm{W}$). While being relatively small, the SBS term cannot be ignored. High differential gains ($G_1/G_2 > 10$) are easily observed, and according to equation (9), any signal, whose input SOP even slightly deviates from that of $\vec{E}_{sig}^{in\_\min}$, will emerge with its SOP being pulled towards that of $\vec{E}_{sig}^{out\_\max}$. While the polarization pulling is due to the SBS term, the final signal SOP is not that of $\vec{E}_{pump}(z=L)$. The relation between the SOP of $\vec{E}_{sig}^{out\_\max}$ and that of $\vec{E}_{pump}(z=L)$ are studied below.

Let us assume first a very weak pump so that the Brillouin term in Eq. (10b) can be ignored. In this limit, the forward evolution of $\hat{s}_{sig}$ and the backward evolution of $\hat{s}_{pump}$ are solely governed by the birefringence term. We denote the maximum value of $\left\langle\hat{s}_{pump}\cdot\hat{s}_{sig}\right\rangle_L$ over all possible SOPs of the input signal $\hat{s}_{sig}(z=0)$, but for a given pump SOP ($\hat{s}_{pump}(z=L)$), as $\max_{\hat{s}_{sig}(z=0)}\left\{\left\langle\hat{s}_{pump}\cdot\hat{s}_{sig}\right\rangle_L\right\}$. It is possible to show that the average projection is given by[29]:

$$\left\langle \hat{s}_{pump}\cdot\hat{s}_{sig}\right\rangle_L \approx \left\langle \hat{s}_{pump}(z)\cdot\hat{s}_{sig}(z)\right\rangle_{\substack{Ensemble\\Average}} = \left\langle \hat{s}^T_{pump}(0)\mathbf{M}^T_{\mathbf{T}^*}(z)\cdot\mathbf{M}_{\mathbf{T}}(z)\hat{s}_{sig}(0)\right\rangle_{\substack{Ensemble\\Average}}$$

$$= \hat{s}^T_{pump}(0)\left\langle \mathbf{M}^T_{\mathbf{T}^*}\cdot\mathbf{M}_{\mathbf{T}}(z)\right\rangle_{\substack{Ensemble\\Average}}\hat{s}_{sig}(0) = \frac{1}{3}\hat{s}^T_{pump}(0)\begin{bmatrix}1 & & \\ & 1 & \\ & & -1\end{bmatrix}\hat{s}_{sig}(0). \qquad (15)$$

Here $\mathbf{M}_{\mathbf{T}}(z)$ and $\mathbf{M}_{\mathbf{T}^*}(z)$ are the Mueller matrices representing $\mathbf{T}(z)$ and $\mathbf{T}^*(z)$, respectively (T stands for transpose), and the fiber is assumed to be long enough so that most z values are much larger than many correlation lengths of the random birefringence. Finally, the ensemble averaged value of $\left\langle \mathbf{M}^T_{\mathbf{T}^*}(z)\cdot\mathbf{M}_{\mathbf{T}}(z)\right\rangle$ was taken from the work by Corsi *et al.*[29].

One can easily conclude from Eq. (15) that $\max_{\hat{s}_{sig}(z=0)}\left\{\left\langle \hat{s}_{pump}\cdot\hat{s}_{sig}\right\rangle_L\right\}$ is 1/3, resulting in a maximum achievable gain coefficient of $(2/3)\gamma_0$ (Eq. 14). This maximum is attained when $\hat{s}_{sig}(z=0)$ is the image of $\hat{s}_{pump}(z=0)$ on the Poincare sphere, with the equatorial plane acting as a mirror, namely: $\hat{s}^{\max}_{1,sig}(0)=\hat{s}_{1,pump}(0)$, $\hat{s}^{\max}_{2,sig}(0)=\hat{s}_{2,pump}(0)$ and $\hat{s}^{\max}_{3,sig}(0)=-\hat{s}_{3,pump}(0)$. This $\hat{s}^{\max}_{sig}(z=0)$ is the normalized Stokes representation of the complex conjugate of the pump Jones vector at $z=0$, namely, $\vec{E}^*_{pump}(z=0)$. Conversely, $\min_{\hat{s}_{sig}(z=0)}\left\{\left\langle \hat{s}_{pump}\cdot\hat{s}_{sig}\right\rangle_L\right\}=-1/3$, corresponding to a minimum gain coefficient of $(1/3)\gamma_0$. This minimum value is attained for $\hat{s}^{\min}_{sig}(z=0)=-\hat{s}^{\max}_{sig}(z=0)$, which is the Stokes space representation of a polarization orthogonal to that of $\vec{E}^*_{pump}(z=0)$, to be denoted by $\vec{E}^{*\perp}_{pump}(z=0)$. It is easily proven from Eqs. (1-2) that for a unitary $\mathbf{T}(z)$ (and ignoring the Brillouin term), if $\vec{E}_{sig}$ and $\vec{E}^*_{pump}$ are a parallel pair at $z=0$, they will continue to be parallel for all $0\le z\le L$, so that $\vec{E}^{out\_\max}_{sig}(z=L)$ has the same polarization as that of $\vec{E}^*_{pump}(z=L)$. These analytically obtained results are no different than the seemingly intuitively-derived conclusions of van Deventer and Boot[22], when carefully noting the difference in the reference frame convention, but both approaches are strictly valid only in the limit of very weak pump power. Nonetheless, numerical simulations of equation (3a) show that the relation between $\vec{E}^{\max}_{sig}$ and $\vec{E}^*_{pump}$ holds in the presence of non-negligible level of pump power[25].

2.3 Polarization-induced distortion in SBS slow light setups

The SBS amplification (or attenuation) of signal waves is frequency dependent. The spectral variations in the signal amplitude gain go hand-in-hand with an acquired optical phase that is frequency-dependent as well. Figure 1 (left) shows the real and imaginary parts of the normalized SBS complex gain coefficient for a CW pump wave: $\gamma(\Delta\omega)/\gamma_0 = 1/(1+j\,2\cdot\Delta\omega/\Gamma_B)$, where $\Delta\omega$ denotes the detuning of the signal wave from the frequency of maximum SBS amplification, and $\Gamma_B/2\pi\approx 30$ MHz is the SBS linewidth[1]. The real and imaginary parts govern the amplitude gain and phase variations of the signal wave respectively.

As can be seen in the figure, the imaginary part of the SBS gain coefficient is nearly linear within the amplification bandwidth. Thus, the spectral phase acquired by signal pulses introduces an effective added group delay[13-20, 26]:

$$\tau = -\frac{P_{pump}L}{2}\frac{\partial}{\partial(\Delta\omega)}\left\{\mathrm{Im}\left[\gamma(\Delta\omega)\right]\right\}\Big|_{\Delta\omega=0}. \qquad (16)$$

The added group delay is positive for amplified Stokes waveforms, and negative for attenuated anti-Stokes pulses. The two phenomena, therefore, fall within the categories of 'slow' and 'fast' light, respectively. Figure 1 (right) shows examples of delayed and advanced signal pulses[13]. The amplitudes of the pulses were all normalized to unity. The added group delay is seen to increase with the SBS amplification. In the previous section, we discussed how the amplification provided by a given pump in a given fiber could vary with the SOP of the input signal. It is therefore anticipated that the group delay obtained in SBS slow and fast light setups would be polarization dependent as well.

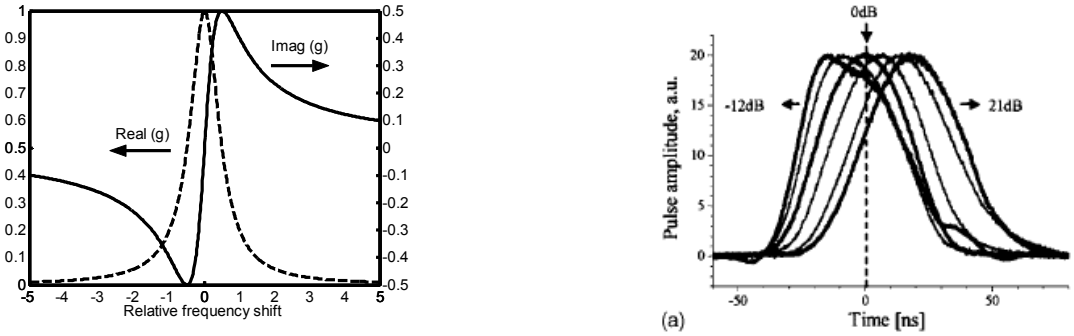

Fig. 1: Left - Schematic real (left hand axis) and imaginary (right hand axis) parts of SBS gain function for CW pump. The frequency is normalized to units of Γ_B. Right - Temporal shift of amplified or attenuated signal pulses[13].

In order to obtain a quantitative description of the polarization dependence of SBS slow light and its implications, let us now consider signal pulses, rather than continuous waves, and denote a single Fourier component of the signal as $\vec{E}_{sig}(z,\Delta\omega)$. Equation (3a) can be re-written for each Fourier component, in the following form:

$$\frac{\mathrm{d}\vec{E}_{sig}(z,\Delta\omega)}{\mathrm{d}z}=\left[\frac{\mathrm{d}\mathbf{T}(z)}{\mathrm{d}z}\mathbf{T}^{\dagger}(z)+\frac{\gamma(\Delta\omega)}{2}\vec{E}_{pump}(z)\vec{E}_{pump}^{\dagger}(z)\right]\vec{E}_{sig}(z,\Delta\omega)\ . \tag{17}$$

The local birefringence term $\left[\mathrm{d}\mathbf{T}(z)/\mathrm{d}z\right]\mathbf{T}^{\dagger}(z)$ is virtually frequency independent within the narrow Γ_B. Repeating the derivation of the previous subsection[30]:

$$\vec{E}_{sig}(L,\Delta\omega)=\mathbf{U}(\Delta\omega)\cdot\begin{bmatrix}G_{\max}(\Delta\omega) & 0\\ 0 & G_{\min}(\Delta\omega)\end{bmatrix}\cdot\mathbf{V}^{\dagger}(\Delta\omega)\cdot\vec{E}_{sig}(0,\Delta\omega)\,, \tag{18}$$

we may obtain the input and output signal SOPs that are associated with maximum and minimum amplification, individually for each Fourier component $\Delta\omega$: $\hat{e}_{sig}^{in\_\max}(\Delta\omega)=\mathbf{V}(\Delta\omega)\cdot\begin{bmatrix}1 & 0\end{bmatrix}^T$, $\hat{e}_{sig}^{in\_\min}(\Delta\omega)=\mathbf{V}(\Delta\omega)\cdot\begin{bmatrix}0 & 1\end{bmatrix}^T$, $\hat{e}_{sig}^{out\_\max}(\Delta\omega)=\mathbf{U}(\Delta\omega)\cdot\begin{bmatrix}1 & 0\end{bmatrix}^T$ and $\hat{e}_{sig}^{out\_\min}(\Delta\omega)=\mathbf{U}(\Delta\omega)\cdot\begin{bmatrix}0 & 1\end{bmatrix}^T$.

In standard, birefringent fibers, $\hat{e}_{sig}^{in\_\max}(\Delta\omega)$ is closely aligned with the complex conjugate of $\vec{E}_{pump}^{*}(0)$ for all $|\Delta\omega|<\Gamma_B$, provided that $\gamma(\Delta\omega)P_{pump}<2\pi/L_B$, where L_B is the mean beat length in the fiber[25]. The input SOPs $\hat{e}_{sig}^{in\_\max}(\Delta\omega)$ and $\hat{e}_{sig}^{in\_\min}(\Delta\omega)$ are therefore nearly frequency independent, even though the maximum and minimum gain values $G_{\max}(\Delta\omega)$, $G_{\min}(\Delta\omega)$ vary exponentially with frequency through $\gamma(\Delta\omega)$. This property of $\hat{e}_{sig}^{in\_\max}(\Delta\omega)$ had been validated by both numerical simulations and experiments[30]. Based on the above, it is possible to replace equation (18) with a pair of decoupled, scalar SBS amplification equations, one associated with the frequency domain transfer function $G_{\max}(\Delta\omega)$ and the input SOP $\hat{e}_{sig}^{in\_\max}(0)$, and the other with $G_{\min}(\Delta\omega)$ and $\hat{e}_{sig}^{in\_\min}(0)$. It is convenient to examine the propagation of an arbitrarily polarized input signal pulse using decomposition in the basis of $\hat{e}_{sig}^{in\_\max}(0)$ and $\hat{e}_{sig}^{in\_\min}(0)$. Since typically $G_{\max}>>G_{\min}$, we expect that the SBS induced delay of a pulse aligned with $\hat{e}_{sig}^{in\_\max}(0)$ will be longer than that of a pulse aligned with $\hat{e}_{sig}^{in\_\min}(0)$. These two SOPs, therefore, take up a role similar to that of the principal axes of linear birefringence induced PMD, on top of representing polarization dependent gain axes[30].

3. EXPERIMENTAL RESULTS

3.1 Stimulated Brillouin scattering polarization pulling

The experimental setup for characterizing polarization related properties of SBS is shown in Fig. 2. Light emitted from a tunable laser source was split by a 50% coupler. In the lower (pump) branch, the light was amplified by a high-power Erbium-doped fiber amplifier (EDFA), and directed into the fiber under test via a circulator. The length of the fiber under test was 2250 m, and its Brillouin frequency shift was ν_B = 10.57 GHz. The pump power was controlled by a variable optical attenuator (VOA). In the upper (signal) branch, the laser light was modulated by an electro-optic intensity modulator (EOM). The modulation frequency was tuned to ν_B, and the EOM bias voltage was adjusted to suppress the optical carrier[4]. Following the EOM, the signal was filtered by a narrow-band Fiber Bragg grating (FBG). For SBS signal amplification measurements, the frequency of the tunable laser was adjusted so that the lower modulation sideband matched the FBG reflection frequency[31]. This way, the frequency of the signal propagating in the fiber under test was ν_B below that of the pump. For SBS attenuation measurements, the tunable laser frequency was modified so that the upper modulation sideband was retained by the FBG[31]. Following the SBS interaction, the signal was routed to a power meter, followed by a lock-in amplifier to filter out spontaneous SBS, or to a polarization analyzer for the measurement of the signal output power and SOP. A second FBG in the detection path was used to filter out the backscattered pump, as well as the spontaneous Brillouin scattering amplified by the Stokes process in the SBS loss scenario.

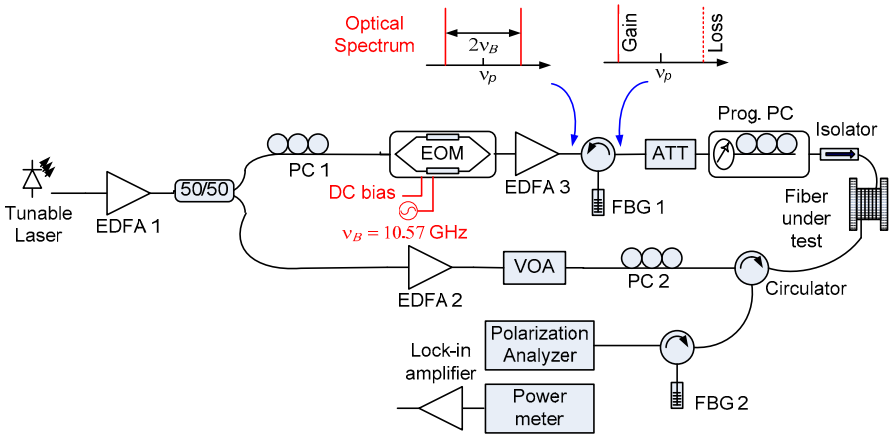

Fig. 2: Experimental setup for characterizing the polarization dependence of SBS. ATT: Optical attenuator. VOA: Variable optical attenuator. FBG: Fiber Bragg grating. DSB: Double side band modulation. SSB: single side band modulation. PC: Polarization controller. EDFA: Erbium-doped fiber amplifier. EOM: electro-optic modulator. ν_p denotes the optical frequency of the pump

For each pump power, the input signal SOPs which corresponded to minimum and maximum signal output power were found using the following procedure: First, a programmable polarization controller (Prog. PC) in the signal path was set to four non-degenerate SOPs, and the output signal power was recorded for each. Based on these four measurements, the top row of the 4X4 Mueller matrix describing the pumped fiber under test was extracted[32], and signal SOPs for minimum and maximum output power could be calculated. Next, the programmable PC was set to these two input SOPs and the output signal power was recorded.

Figure 3(a) shows the logarithm of the signal power gain (Stokes signal) as a function of pump power, for three different SOPs of the input signal wave. In the upper and lower curves, the signal SOP is adjusted for each pump power level to achieve maximum and minimum gain, respectively. In these curves, the logarithmic SBS gain appears to be linearly proportional to the pump power over the entire measurement range, indicating a power-independent gain coefficient, as predicted by the analysis. Furthermore, the slope of the maximum gain curve is extremely close to twice that of the minimum gain curve[22]. These results indicate that our 2.2km fiber comprises many correlation lengths of the random birefringence[22, 29]. The third curve of Fig. 3(a) shows the logarithm of the SBS gain for a signal, whose input SOP, $\vec{E}^{in\_near\_min}_{sig(Stokes)}$, is azimuthally 40° away from $\vec{E}^{in\_min}_{sig(Stokes)}$. Initially, for relatively low pump power, the gain slope is that of the

minimum gain curve. However, for higher pump powers, the measured gain increases rapidly and its slope approaches that of the maximum gain curve.

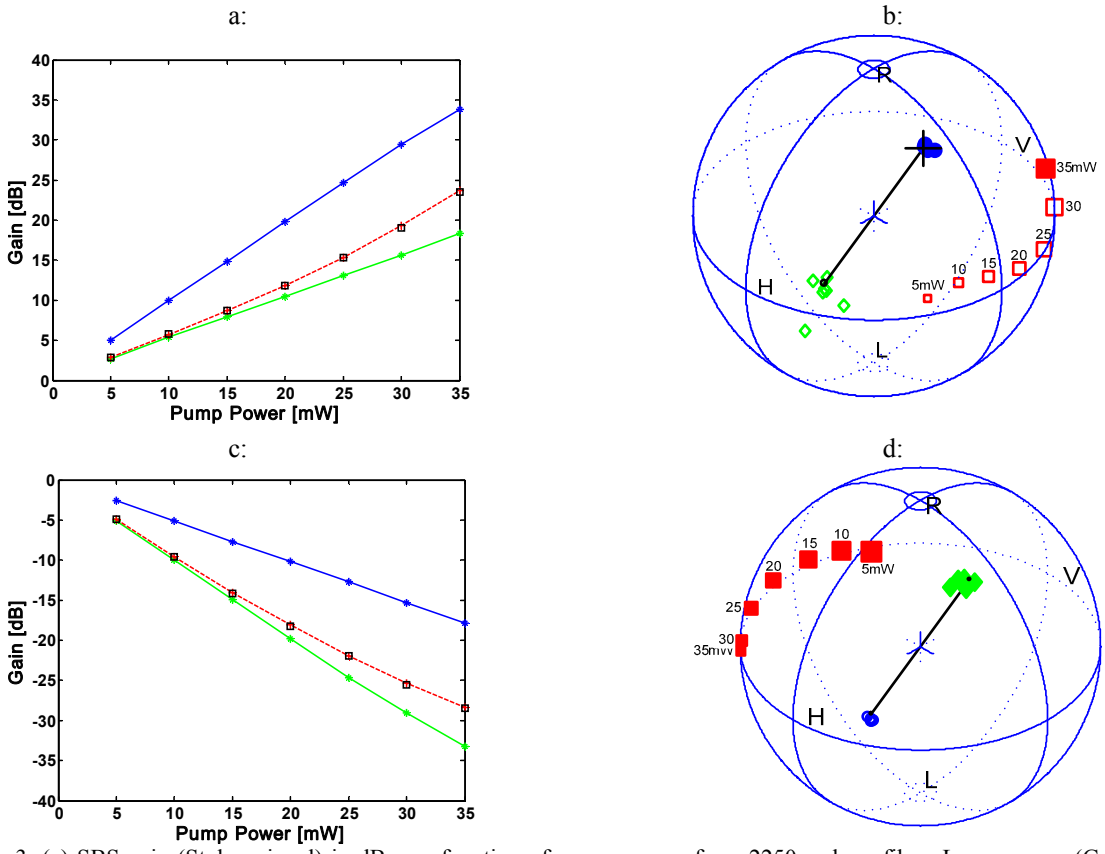

Fig. 3: (a) SBS gain (Stokes signal) in dB as a function of pump power, for a 2250 m long fiber. Lower curve (Green) – optimized for minimum gain, Upper curve (Blue) – optimized for maximum gain, Dashed curve (Red) – for an input SOP in the vicinity of $\vec{E}_{sig(Stokes)}^{in\_\min}$, rotated from it by 40^0 around the s_3 (RL) axis (the black squares are explained in the text). (b) The SOPs of the emerging amplified signals for the three cases of (a): maximum (blue solid circles), minimum (green open diamonds), and red squares for the intermediate case. Open symbols denote SOPs in the back of the sphere. The size of the square is a measure of the signal power, *increasing* with pump power for Stokes signals. The black '+' is the SOP of the spontaneous SBS. The straight line through the center of the sphere connects this SOP to its orthogonal counterpart. (c) SBS attenuation (anti-Stokes signal) in dB as a function of pump power. Lower curve (Green) – optimized for minimum output power (maximum attenuation), Upper curve (Blue)– optimized for maximum output power (minimum attenuation), Dashed curve (Red) – for an input SOP in the vicinity of $\vec{E}_{sig(A-Stokes)}^{in\_\min}$, rotated from it by 40^0 around the s_3 (RL) axis. (d) The SOPs of the emerging attenuated signals for the cases of (c): maximum (blue open circles), minimum (green solid diamonds), and red squares for the intermediate case. The straight line through the center of the sphere is that of (b), shown here for reference.

As a consistency check, we used Eqs. (8)-(9) first to project $\vec{E}_{sig(Stokes)}^{in\_near\_\min}$ on the measured $\vec{E}_{sig(Stokes))}^{in\_\max}$, $\vec{E}_{sig(Stokes)}^{in\_\min}$, and then used the measured values for G_1 (maximum gain) and G_2 (minimum gain) to analytically predict the gain experienced by $\vec{E}_{sig(Stokes))}^{in\_near\_\min}$. The results are shown as open squares on the dashed (red) curve in Fig. 3(a), demonstrating excellent agreement with the measured gain. Figure 3(b) shows the output SOPs corresponding to $\vec{E}_{sig(Stokes)}^{out\_\max}$, $\vec{E}_{sig(Stokes)}^{out\_\min}$ and $\vec{E}_{sig(Stokes)}^{out\_near\_\min}$ for all pump powers. Also shown on the sphere is the SOP of spontaneously amplified Brillouin scattering, which was obtained by turning off the signal input and measuring the SOP of the Brillouin-scattered light at $\nu_s = \nu_p - \nu_B$. Note that as P_{pump} spans the 5-35mW range, $\{\vec{E}_{sig(Stokes)}^{out\_\max}\}$ and $\{\vec{E}_{sig(Stokes)}^{out\_\min}\}$ hardly change and they are fairly orthogonal to one another (the SOP readings of the polarization analyzer in the minimum gain case were contaminated

by the spontaneously amplified Brillouin scattering, leading to a larger spread near $\left\{\vec{E}_{sig(Stokes)}^{out\_\min}\right\}$). Furthermore, $\left\{\vec{E}_{sig(Stokes)}^{out\_\max}\right\}$ coincides, as expected, with the SOP of the spontaneously amplified Brillouin scattering. Also shown is the evolution of the signal SOP for $\vec{E}_{sig(Stokes)}^{in\_\text{near}\_\min}$, clearly indicating the pulling of its SOP towards that of $\left\{\vec{E}_{sig(Stokes)}^{out\_\max}\right\}$. Figure 3(c) shows the logarithm of the maximum and minimum attenuation of an anti-Stokes signal. As obtained for the Stokes wave, the curves for maximum and minimum are linear, and the ratio of their slopes is close to two. Note that the obtained curves replicate those of the corresponding Stokes signal, albeit with a minus sign. The figure also shows the measured and calculated logarithmic loss of an anti-Stokes signal with an input SOP $\vec{E}_{sig(A-stokes)}^{in\_\text{near}\_\min}$. Finally, Fig. 3(d) shows the output SOPs corresponding to $\vec{E}_{sig(A-Stokes)}^{out\_\max}$, $\vec{E}_{sig(A-Stokes)}^{out\_\min}$ and $\vec{E}_{sig(A-Stokes)}^{out\_\text{near}\_\min}$ for all pump powers. Polarization pulling towards the SOP of $\left\{\vec{E}_{sig(A-Stokes)}^{out\_\max}\right\}$ is observed. It is seen that $\left\{\vec{E}_{sig(A-Stokes)}^{out\_\min}\right\}$ (solid diamonds in Fig. 3(d)), which suffers maximum attenuation are parallel to $\left\{\vec{E}_{sig(Stokes)}^{out\_\max}\right\}$ (solid circles in Fig. 3(b)), which enjoys the maximum possible gain.

Figure 4 shows the signal output SOP for twenty different input SOPs, which were evenly distributed on the Poincare sphere. As the pump power is increased, the output signal SOPs converge to a particular, preferred state. The convergence is effective for both SBS signal gain and signal loss, in the undepleted pump regime.

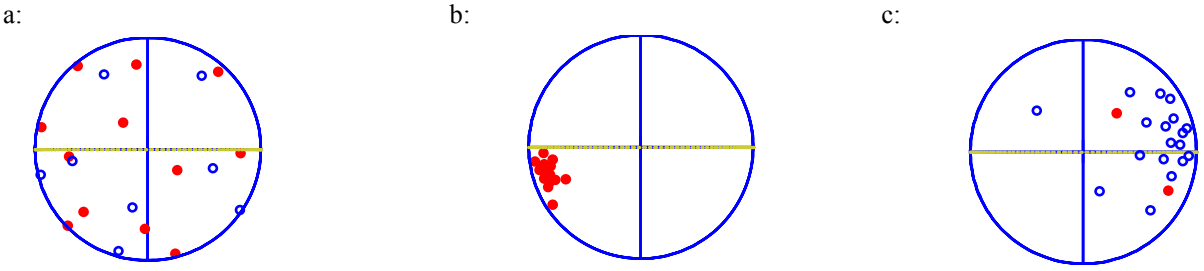

Fig. 4: Measured output signal SOP for SBS signal gain and SBS signal loss for twenty evenly distributed input signal SOPs. (a) Stokes SOP, pump power is 5 mW. (b) Stokes SOP, pump power is 45 mW. (c) Anti-Stokes SOP, pump power is 20mW (SOP measurements in the signal attenuation scenario were difficult due to the presence of spontaneous SBS, which competed with the attenuated signal. Thus, reliable readings could not be obtained for pump powers above 25 mW.)

3.2 Polarization-induced distortion in SBS slow light

Excessive polarization-related pulse broadening was observed experimentally. The measurement setup is shown in Fig. 5. Light from a distributed feedback laser diode (DFB-LD) was split by a directional coupler. One branch was amplified using an EDFA, and was launched into the fiber under test as an SBS pump wave at $z = L$. The other branch was double-sideband modulated at the Brillouin frequency shift of the fiber under test (10.91 GHz), with the bias of the EOM adjusted to suppress the optical carrier frequency. The upper frequency sideband was discarded by a narrowband FBG, and the filtered lower frequency sideband was used as a Stokes wave signal. This signal was then modulated by Gaussian pulses, using a second EOM, and was launched into the fiber at $z = 0$. A PC was used to adjust the input signal SOP. The pump power, fiber length and input pulse full width at half maximum (FWHM) were 560 mW, 140 m and 17 ns.

Figure 6 shows measurements of the normalized output power for different input SOPs. The gain and FWHM of maximally amplified output pulse power $P_{sig}^{out\_\max}(t)$ were 21 dB and 63 ns, whereas those of the minimally amplified pulse power $P_{sig}^{out\_\min}(t)$ were 6.7 dB and 30 ns. Several pulses of intermediate SOP alignments, amplified by only 9.5-13 dB, were broadened to a FWHM of 65-75 ns. The results demonstrate that SBS slow light implementations may introduce a polarization-related distortion, which is inherent to the vector nature of SBS. Polarization induced distortion becomes negligible when the signal input is closely aligned with $\hat{e}_{sig}^{in\_\max}(0)$, which is the preferable input SOP in most slow light setups. Nonetheless, our results show that an arbitrarily polarized signal pulse, subject to a comparatively moderate amplification, can become broader than a pulse aligned for maximum gain and delay. Unless polarization is stabilized, the width of the maximally delayed pulse does not necessarily set an upper bound on pulse broadening in SBS slow light delay setups.

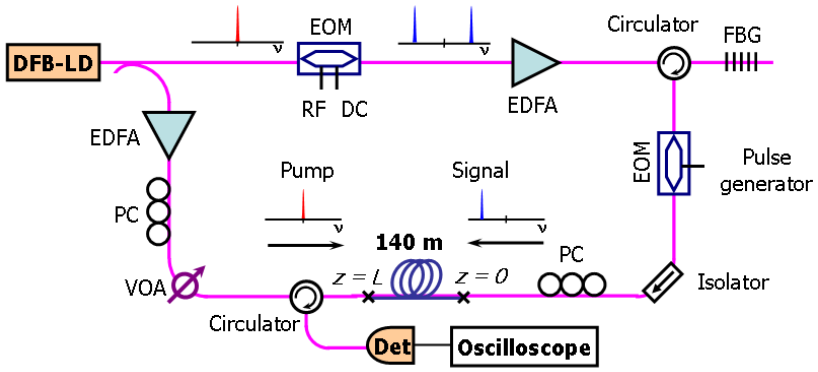

Fig. 5: Experimental setup for observing SBS-PMD. VOA: variable optical attenuator. Det: detector. RF: radio frequency. DC: direct current.

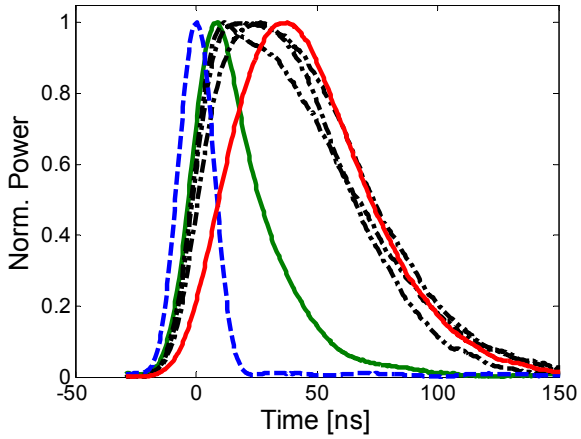

Fig. 6: Measured, normalized signal power as a function of time. Dashed line (blue): input Gaussian pulse (FWHM 17 ns). Solid lines: output pulses with the input SOP aligned for minimum gain (left, green) and maximum gain (right, red). Dash-dot lines (black): examples of output pulses with intermediate input SOP alignments. Experimental conditions: L =140 m, P_{pump} = 560 mW.

4. DISCUSSION AND CONCLUSIONS

In this work, the analysis of SBS in birefringent fibers was extended to include arbitrarily polarized signals. A vector propagation equation for the signal wave in the undepleted pump regime was provided, both in Jones and in Stokes spaces. The equations and their subsequent analysis provide expressions for the output signal vector, regardless of the polarization statistics of the pump and signal waves along the fiber. The analysis showed that SBS in the undepleted pump regime may be modeled as a pseudo-linear partial polarizer, whose input states for maximum and minimum gain are orthogonal. Due to the large difference in gain between these maximum and minimum states, it is expected that the SOP of an arbitrarily polarized input signal will be closely aligned with that of the maximum gain axis at the fiber output. This prediction was experimentally confirmed, for both Stokes and anti-Stokes signal waves. The vector properties of SBS can give rise to an arbitrary polarization synthesis. The analysis also shows that the maximum and minimum input signal SOPs for the Stokes wave in long, standard single-mode fibers correspond to the conjugate of the outgoing pump, and the orthogonal of that conjugate, respectively. This correspondence is practically valid for pump powers up to tens of mW over fibers a few km long. The roles of the two SOPs are reversed for the anti-Stokes wave.

The polarization and birefringence dependence of SBS has already been used in Brillouin fiber lasers[33, 34] and distributed birefringence measurements[35]. On the other hand, the same dependence can hinder the performance of distributed strain and temperature sensors[36]. In addition, birefringence was observed to cause a nonlinear response in the delay-pump

power transfer function[37]. In another example, the polarization sensitivity of SBS-induced delay was overcome using a Faraday rotator mirror[38]. The quantitative analysis of the strength of polarization pulling over relatively short spans of standard fibers could provide information regarding the beat length and polarization coupling length of a specific fiber under test[39]. Finally, frequency-selective polarization pulling based on SBS was recently applied in the generation of orthogonally polarized, optical single-sideband modulation formats[40]. Polarization properties of SBS are also addressed in the works of Galtarossa *et al.*[41] and Ursini *et al.*[42]. Clearly, the research interest in the polarization attributes of SBS in optical fibers and their applications is on the rise. Nonlinear polarization pulling based on stimulated Raman scattering amplification[43] and the Kerr effect[44, 45] were also demonstrated over the last two years.

Polarization induced distortion becomes negligible when the signal input is closely aligned with the SOP of maximum delay, which is the preferable input state in most slow light setups. For this reason, the effect was seldom encountered by researchers working on SBS slow light setups. Nonetheless, our results show that an arbitrarily polarized signal pulse, subject to a comparatively moderate amplification, can become broader than a pulse aligned for maximum gain and delay. Unless polarization is stabilized, the width of the maximally delayed pulse does not necessarily set an upper bound on pulse broadening in SBS slow light delay setups.

REFERENCES

[1] Boyd, R. W., [Nonlinear optics], Academic Press, San Diego, CA, chapter 9, 409-427, (2003).
[2] Yariv, A. [Optoelectronics], 4th Edition, Saunders College Publishing, Orlando, FL, chapter 19, 670-678, (1991).
[3] Horiguchi, T., Kurashima, T., and Tateda, M., "A technique to measure distributed strain in optical fibers," IEEE Photon. Technol. Lett. 2, 352-354, (1990).
[4] Nikles, M., Thévenaz, L., and Robert, P., "Brillouin gain spectrum characterization in single-mode optical fibers," J. Lightwave Technol. 15, 1842-1851, (1997).
[5] Bao, X., Webb, D. J., and Jackson, D. A., "32-km distributed temperature sensor using Brillouin loss in optical fiber," Opt. Lett. 18, 1561-1563, (1993).
[6] Yong, J. C., Thévenaz, L., and Kim, B. Y., "Brillouin fiber laser pumped by a DFB laser diode," J. Lightwave Technol. 12, 546-554, (2003).
[7] Loayssa, A., Benito, D., and Grade, M. J., "Optical carrier-suppression technique with a Brillouin-erbium fiber laser," Opt. Lett. 25, 197-199, (2000).
[8] Shen, Y., Zhang, X., and Chen, K., "Optical single side-band modulation of 11 GHz RoF system using stimulated Brillouin scattering," IEEE Photon. Technol. Lett. 17, 1277-1279, (2005).
[9] Zadok, A., Eyal, A., and Tur, M., "GHz-wide optically reconfigurable filters using stimulated Brillouin scattering," J. Lightwave Technol. 25, 2168-2174, (2007).
[10] Loayssa, A. and Lahoz, F. J., "Broadband RF photonic phase shifter based on stimulated Brillouin scattering and single side-band modulation," IEEE Photon. Technol. Lett. 18, 208-210, (2006).
[11] Loayssa, A., Capmany, J., Sagues, M., and Mora, J., "Demonstration of incoherent microwave photonic filters with all-optical complex coefficients," IEEE Photon. Technol. Lett. 18, 1744-1746, (2006).
[12] Zhu, Z., Gauthier, D. J., and Boyd, R. W., "Stored light in an optical fiber via Stimulated Brillouin Scattering," Science 318, 1748-1750, (2007).
[13] González-Herráez, M., Song, K.-Y., and Thévenaz, L., "Optically controlled slow and fast light in optical fibers using stimulated Brillouin scattering," Appl. Phys. Lett. 87, 081113, (2005).
[14] Stenner, M. D., Neifeld, M. A., Zhu, Z., Dawes, A. M. C., and Gauthier, D. J., "Distortion management in slow-light pulse delay," Opt. Express 13, 9995-10002, (2005).
[15] Zhu, Z., Dawes, A. M. C., Gauthier, D. J., Zhang, L., and Willner, A. E., "Broadband SBS slow light in an optical fiber," J. Lightwave Technol. 25, 201-206, (2007).
[16] González-Herráez, M., Song, K.-Y., and Thévenaz, L., "Arbitrary-bandwidth Brillouin slow light in optical fibers," Opt. Express 14, 1395-1400, (2006).
[17] Song, K. Y., Gonzalez Herraez, M., and Thévenaz, L., "Observation of pulse delay and advancement in optical fibers using stimulated Brillouin scattering," Opt. Express 13, 82-88, (2005).
[18] Zadok, A., Eyal, A., and Tur, M., "Extended delay of broadband signals in stimulated Brillouin scattering slow light using synthesized pump chirp," Opt. Express 14, 8498-8505, (2006).

[19] Thévenaz, L., "Slow and fast light in optical fibers," Nature Photonics 2, 474-481 (2008).
[20] Gehring, G. M., Boyd, R. W., Gaeta, A. L., Gauthier, D. J., and Willner, A. E., "Fiber-based slow-light technologies," J. Lightwave Technol. 26, 3752-3762 (2008).
[21] Horiguchi, T., Tateda, M., Shibata, M., and Azuma, Y., "Brillouin gain variation due to a polarization-state change of the pump or Stokes field in standard single mode fibers," Opt. Lett. 14, 329-331, (1989).
[22] van Deventer, M. O. and Boot, A. J., "Polarization properties of stimulated Brillouin scattering in single mode fibers," J. Lightwave Technol. 12, 585-590, (1994).
[23] Jones, R. C., "A new calculus for the treatment of optical system," J. Opt. Soc. Am. 37, 107-110, (1947).
[24] Collett, E., Editor, [Polarized light fundamentals and applications], Marcel Dekker, New York, (1993).
[25] Zadok, A., Zilka, E., Eyal, A., Thévenaz, L., and Tur, M., "Vector analysis of stimulated Brillouin scattering amplification in standard single-mode fibers," Opt. Express 16, 21692-21707 (2008).
[26] Zhu, Z., Gauthier, D. J., Okawachi, Y., Sharping, J. E., Gaeta, A. L., Boyd, R. W., and Willner, A. E., "Numerical study of all-optical slow-light delays via stimulated Brillouin scattering in an optical fiber," J. Opt. Soc. Am. B 22, 2378-2384 (2005).
[27] Gordon, J. P. and Kogelnik, H., "PMD fundamentals: polarization mode dispersion in optical fibers", P. Natl. Acad. Sci. USA 97, 4541-4550, (2000).
[28] Stolen, R. H., "Polarization effects in fiber Raman and Brillouin lasers," IEEE J. of Quantum Electron. 15, 1157-1160, (1979).
[29] Corsi, F., Galtarossa, A., and Palmieri, L., "Analytical treatment of polarization mode dispersion in single mode fibers by means of the backscattered signal," J. Opt. Soc. Am. A 16, 574-583, (1999).
[30] Zadok, A., Chin, S., Thevenaz, L., Zilka, E., Eyal, A., and Tur, M., "Polarization induced distortion in stimulated Brillouin scattering slow light systems," Opt. Lett., 34, 2530-2532, (2009).
[31] Loayssa, A., Benito, D., and Grade, M. J., "High resolution measurement of stimulated Brillouin scattering spectra in single-mode fibers," IEE Proc. Optoelectron. 148, 143-148, (2001).
[32] Eyal, A., Kuperman, D., Dimenstein, O., and Tur, M., "Polarization dependence of the intensity modulation transfer function of an optical system with PMD and PDL," IEEE Photon. Technol. Lett. 14, 1515-1517, (2002).
[33] Küng, A., Thévenaz, L., and Robert, P. A., "Polarization analysis of Brillouin scattering in a circularly birefringent fiber ring resonator," J. Lightwave. Technol. 15, 977-982, (1997).
[34] Randoux, S., Zemmouri, J., "Polarization dynamics of a Brillouin fiber ring laser," Phys. Rev. A 59, 1644-1653, (1999).
[35] Thévenaz, L., Foaleng Mafang, S., and Nikles, M., "Fast measurement of local PMD with high spatial resolution using stimulated Brillouin scattering," paper 10.1.2 in ECOC 2007, Berlin, Germany, (2007).
[36] Bao, X., Dhliwayo, J., Heron, N., Webb, D. J., and Jackson, D. A., "Experimental and theoretical studies on a distributed temperature sensor based on Brillouin scattering," J. Lightwave Technol. 13, 1340-1348, (1995).
[37] Chin, S., Gonzalez-Herraez, M., and Thévenaz, L., "Zero-gain slow and fast light propagation in an optical fiber," Opt. Express 14, 10684-10692, (2006).
[38] Walker, D. R., Bashkanski, M., Gulian, A., Fatemi, F. K., and Steiner, M., "Stabilizing slow light delay in stimulated Brillouin scattering using a Faraday rotator mirror," J. Opt. Soc. Am. B **25**, C61-C64 (2008).
[39] Zadok, A., Zilka, E., Eyal, A., Thevenaz, L., and Tur, M., "Fiber beat length estimates via polarization measurements of stimulated Brillouin scattering amplified signals," paper OMP4 in OFC/NFOEC 2009, San Diego, Ca, 2009.
[40] Sagues, M., and Loayssa, A., "Orthogonally polarized optical single sideband modulation for microwave photonics processing using stimulated Brillouin scattering," Opt. Express 18, 22906-22914, (2010).
[41] Galtarossa, A., Palmieri, L., Santaguistina, M., Schenato, L., and Ursini, L., "Polarized Brillouin amplification in randomly birefringent and unidirectionally spun fibers," IEEE Photon. Technol. Lett. 20, 1420-1422 (2008).
[42] Ursini, L., Santagiustina, M., and Palmieri, L., "Polarization-Dependent Brillouin Gain in Randomly Birefringent Fibers," IEEE Photon. Technol. Lett. 22(10), 712-714 (2010).
[43] Martinelli, M., Cirigliano, M., Ferrario, M., Marazzi, L., amd Martelli, P., "Evidence of Raman-induced polarization pulling," Opt. Express 17, 947-955 (2009).
[44] Pitois, S., Fatome, J., and Millot, G., "Polarization attraction using counterpropagating waves in optical fiber at telecommunication wavelengths," Opt. Express 16, 6646-6651 (2008)
[45] Fatome, J., Pitois, S., Morin, P., and Millot, G., "Observation of light-by-light polarization control and stabilization in optical fibre for telecommunication applications," Opt. Express 18, 15311-15317 (2010)